Roadside Seismic Survey Utilizing Traffic Noise

Choon B. Park*, Richard D. Miller*, and Nils Ryden[+]

**Kansas Geological Survey, The University of Kansas, Lawrence, Kansas, USA*
[+]Dep. of Engineering Geology, Lund Institute of Technology, Sweden

Abstract

Traffic-generated seismic waves mainly consist of Rayleigh-type surface waves whose dispersion property can be used to deduce shear-wave velocity (Vs) information of near-surface (< 100m) materials. Although, for the most accurate results, a 2D receiver array such as a cross or circular type should be used in this type of passive surface wave survey, it is often not possible to secure such a spacious area especially if the survey has to take place in an urban area. A passive version of the multichannel analysis of surface waves (MASW) method can be implemented with the conventional linear receiver array deployed alongside a road. Offline, instead of inline, nature of source points on the road is accounted for by a dispersion analysis scheme that makes no assumption on the incoming angle (azimuth) of surface waves. Circular, instead of planar, nature of wavefront that often occurs due to the proximity of source points is also accounted for by considering the distance between a receiver and a possible source point. The processing schemes are compared in performance to the one that accounts for inline propagation only. Comparisons made with field data sets showed that the latter scheme can result in overestimation of phase velocities up to 30 percent, whereas the overestimation can be reduced to less than 10 percent if the proposed schemes are used.

INTRODUCTION

As the necessity of surveys inside urban areas grows and the active survey mode often does not achieve sufficient depth of investigation, the passive surface wave method utilizing those surface waves generated by local traffic is deemed to be a fascinating choice recently (Louie, 2001; Okada, 2003; Yoon and Rix, 2004; Park et al., 2004). Furthermore, because the true 2D receiver array such as a cross layout is not a practical or possible mode of survey in urban areas populated with buildings, a method that can be implemented with the conventional 1D linear receiver array should get its own credit in any case (Louie, 2001). The underlying assumption with such a 1D method lies in the nature of wave propagation which is the same inline propagation as in the case of an active survey. Subsequent data processing for dispersion analysis is therefore a 1D

scheme considering only those waves propagating parallel to (inline with) the linear receiver line.

In the case of a passive survey alongside a road, points of surface wave generation are usually on the road since waves are generated when moving vehicles travel onto irregularities on the road. Because the receiver line is always off the surveying road and there are other roads in the area, the wave propagation is therefore hardly in accordance with the inline propagation although being close to it when sources are at far distances on a straight surveying road. If those strong waves from nearby source points dominate and their offline nature is not accounted for during the dispersion analysis, phase velocities are overestimated approximately in inverse proportion to the cosine of the azimuth ($\cos\theta$). Furthermore, considering relatively strong energy from nearby source points, the dominating mode of propagation may be not only offline but also non-planar with a wavefront whose curvature cannot be ignored.

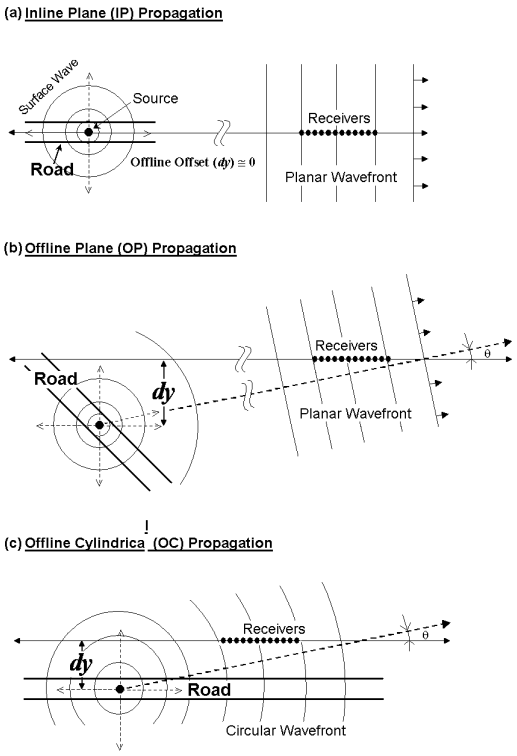

Fig. 1 Three different types of possible wave propagation with a roadside surface wave method with a 1-D linear receiver arrav.

Ways to account for these offline source points and circular wavefront are described with results compared to those from the conventional analysis scheme based on the inline plane wave propagation (Louie, 2000). Fundamentals of data acquisition and processing techniques have evolved from the multichannel analysis of surface waves (MASW) method for active surface wave surveys (Park et al., 1999).

ROADSIDE PASSIVE SURFACE WAVES

Three different types of wave propagation can exist: inline plane (IP), offline plane (OP), and offline cylindrical (OC) propagations (Fig. 1). Propagation of waves generated from distant points on the surveying road (for example, at a distance 10 times or more array lengths) can be an example of the IP type if the road is fairly straight in the corresponding segment (Fig. 1a). On the other hand, if the road turns or there are other roads around the surveying area, there can be waves generated at far distances approaching the receiver line with a significant azimuthal angle making an example of the OP type (Fig. 1b). Furthermore, source points on the surveying road can be close to the array (for example, at a distance shorter than a few times array length from either end or even within the receiver line), making an example of the OC type (Fig. 1c). Waves of OC type propagate into the receiver line with a significant curvature due to the proximity and the offline nature. A considerable amount of recorded energy can be of this origin due to relatively strong source energy.

SCHEMES FOR DISPERSION IMAGING

Dispersion imaging schemes to deal with each of these types of propagation are described. It is assumed that the road runs along the horizontal axis (x) with the receiver line in parallel to it.

Inline Plane (IP) Waves

IP waves are the simplest type from the data processing perspective. They can be processed by any scheme commonly used for active surveys. With the scheme by Park et al. (1998; 2004), to calculate the relative energy, $E_{IP}(\omega,c)$, for a particular frequency ($\omega=2\pi f$) and a scanning phase velocity (c) in the dispersion image, it first applies the necessary phase shift ($\phi_i=\omega x_i/c$) to the Fourier transformation, $R_i(\omega)$, of the *i-th* trace, $r_i(t)$, at offset x_i, sums all (N) phase-shifted traces, and then takes the absolute value of the summed complex number:

$$E_{IP}(\omega,c)=\left|\sum_{i=1}^{N} e^{j\phi_i} R_i(\omega)\right|+\left|\sum_{i=1}^{N} e^{-j\phi_i} R_i(\omega)\right| \qquad (1)$$

To account for the possible bidirectional nature of the incoming waves from both ends of the receiver array, the step of phase shift followed by the summation is repeated by changing the sign of the phase shift in the above equation. A method by Louie (2001)—commonly known as the refraction microtremor (ReMi) method—is based on this algorithm in its data-processing principles by assuming that the major part of the

recorded waves are of IP type and any other offline waves of significant energy, if they exist, should appear at higher phase velocities. It therefore tries to extract a curve by following a trend of lowest phase velocity in the energy band of dispersion in the space of $E_{IP}(\omega,c)$. With this method, however, the consideration of the inherent banding effect in imaging due to the limited spatial coverage of the measurement is not properly accounted for. This is illustrated in Fig. 2 where images of a constant phase velocity (500 m/sec) are displayed that were obtained by using the scheme (1) from IP cases with two different receiver array lengths (23 m and 92 m). This modeling with a perfectly inline source illustrates the inherent band appearance of the image resulting from finite lengths in time (t) and space (x). It is also noticed that width of the band changes with wavelength.

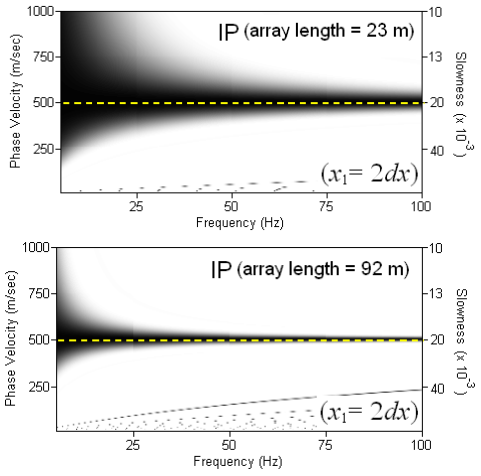

Fig. 2 Dispersion images processed from synthetic records modeling a perfectly inline source by using the IP scheme. Two different receiver array lengths are considered.

Offline Plane (OP) Waves

OP waves can be processed by any algorithm based on the conventional 2D wavenumber (k_x-k_y) method (Lacoss et al., 1969). The method by Park et al. (2004) modifies the traditional method in such a way that the possible multi-modal nature of dispersion can be imaged in an intuitive manner by stacking energy in the 2D wavenumber space along the azimuth axis. This method therefore adds another parameter for scanning in comparison to (1): the azimuth (θ). For each frequency (ω), the energy, $E_{OP}(\omega,c,\theta)$, for a scanning phase velocity (c) is calculated by assuming an azimuth (θ). This calculation is then carried over the scanning range of the phase velocity (for example, 50 m/sec-3000 m/sec with 5-m/sec increment), and then over that of the azimuth (for example, 0-180 degrees in 5-degree increments):

$$E_{OP}(\omega,c,\theta)=\left|\sum_{i=1}^{N} e^{j\phi_{\theta,i}} R_i(\omega)\right| \quad (\text{for } 0^\circ \le \theta \le 180^\circ) \qquad (2)$$

For given c and θ, the necessary phase shift $\phi_{\theta i}$=-$\omega x_i \cos\theta/c$ for a trace at x_i is calculated based on the projection principle (Park et al., 2004). Here the scanning range of azimuth (θ) is only within the two quadrants (180 degrees) due to the linear nature of the receiver line. All the IP waves that exist are handled in a correct manner as they are detected during the scanning of azimuth near 0 and 180 degrees, respectively.

Offline Cylindrical (OC) Waves

OC waves are processed in a similar manner to the OP waves, (2), only with an additional consideration of the finite, rather than infinite, distance ($l_{\theta,i}$) between the source point (x_θ, y_θ) and each receiver point (x_i) for a scanning angle θ (Fig. 3):

$$l_{\theta,i} = \sqrt{(x_\theta - x_i)^2 + y_\theta^2} \qquad (\text{with } x_\theta = y_\theta / \tan\theta \text{ and } y_\theta = dy) \tag{3}$$

Then, the phase shift term in equation (2) is determined as $\phi_{\theta i}$=-$\omega l_{\theta i}/c$. The distance, $l_{\theta,i}$, obviously can change as the road itself has its own width and irregularities may exist anywhere on the road. An extensive modeling experiment indicated that the exact distance, however, is not critical and that the distance between the center of the road and the receiver line is usually sufficient enough to account for the curvature in the arrival pattern of the OC waves. This scheme processes the IP waves correctly as it becomes identical to that for the IP waves for grazing azimuthal angles (close to 0 or 180 degrees). OP waves (for example, waves from other nearby roads) can also be processed by this scheme, only with a slightly reduced sensitivity.

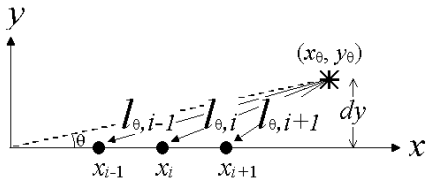

Fig. 3 A schematic illustration of how the offline cylindrical waves are accounted for during the scanning of an azimuth (θ).

FIELD DATA EXAMPLE

Two sets of field data were used to test these three processing schemes. One data set (OCT-03) was prepared from the data set acquired in October 2003 (Park et al., 2004) near a soccer field in Lawrence, Kansas, by using a 2D cross layout of total 48 channels (Fig. 4a) with a 5-m receiver spacing. The first 24-channel data that ran East-West (E-W) in parallel to the Clinton Parkway were taken to mimic a 1D linear array. The separation (dy) between this receiver line and the center of Clinton Parkway was about 100 meters. For comparison purposes, a dispersion image obtained from the full data set

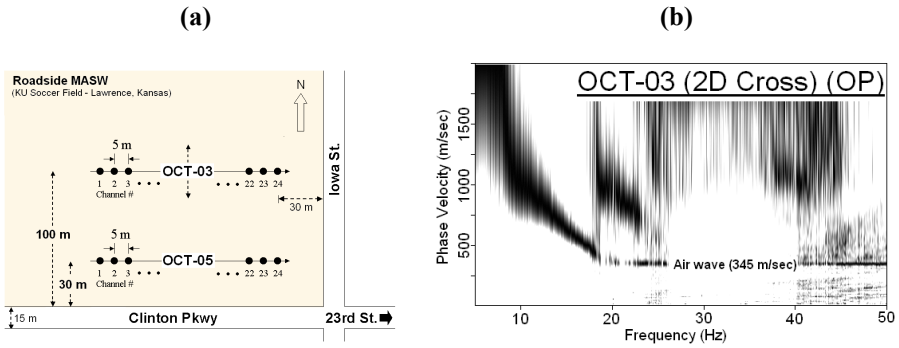

Fig. 4 (a) Map showing field layouts for two experiments performed during October of 2003 (OCT-03) and 2005 (OCT-05). A 48-channel 2D cross receiver array was used for the earlier experiment, whereas a 24-channel linear array was used during the later survey. (b) Dispersion image processed from the 48-channel 2D array records by using the offline plane (OP) scheme.

of the 2D cross layout has been displayed in Fig. 4b. The other set of data (OCT-05) was acquired in October 2005 using a 24-channel linear array directly south of the E-W line used for OCT-03 by using the same receiver spacing of 5 meters (Fig. 4). This line was about 30 meters from the road (*dy* = 30 m).

Ten individual records acquired at each survey time were processed using three different schemes, and their dispersion images were vertically stacked together (to increase the image resolution) to make the images displayed in Fig. 5. The strong major trend of dispersion visible on all images in 8-17 Hz was previously confirmed as a higher mode (M1), instead of the fundamental mode (M0), through a combined analysis with an active survey (Park et al., 2005). Dispersion curves were extracted from the trends by picking maximum points in the energy band with a small interval (0.01 Hz) and then calculating the best fitting curve through the linear regression method. All these curves are displayed in Fig. 5d and Fig. 6. Curves from the IP scheme show overestimations in comparison to those from the other two schemes in both surveys. The amount of overestimation, however, becomes smaller as the receiver array gets closer to road (Fig. 6). It is also shown that the two offline (OP and OC) schemes resulted in a certain amount of overestimation for frequencies lower than 12 Hz (for wavelengths longer than about 75 meters) as noticed when compared to the curve from a 2D cross layout. Curves from the survey closer to the road show (OCT-05) a slight difference in general trend, possibly due to a slight difference in near-surface geology in comparison to the results from the previous survey performed about 70-meters further away.

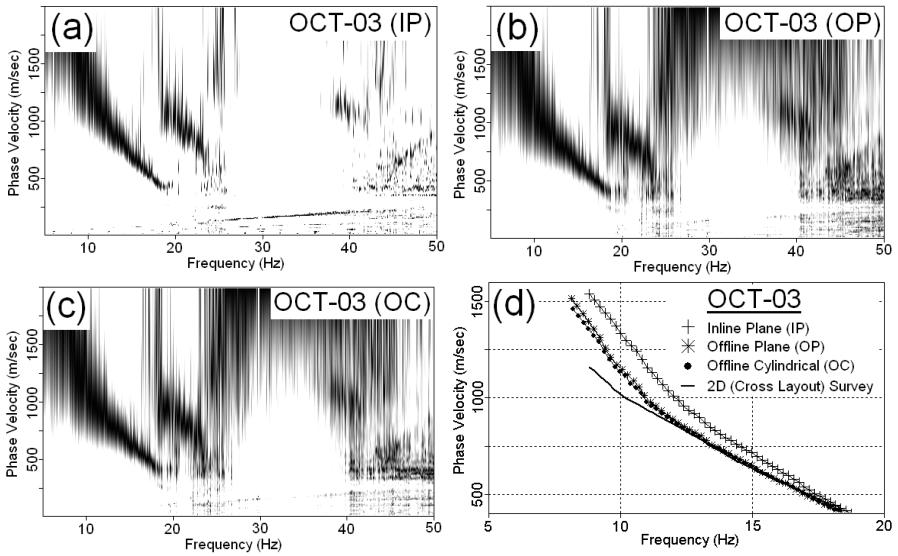

Fig. 5 Dispersion images processed from 24-channel records along the E-W line used during the field experiment in October 2003, obtained by using (a) IP, (b) OP, (c) OC schemes, and (d) curves extracted from the major energy trend.

DISCUSSIONS

Because the relative dominance of each type of waves cannot be known in advance, using the OC scheme is recommended if the road is fairly straight for a significant distance without any other major roads intersecting or passing nearby. The OP scheme may also be applied for comparison purposes. The IP scheme can be a convenient tool for a quick in-field quality control purpose, as it is the fastest scheme.

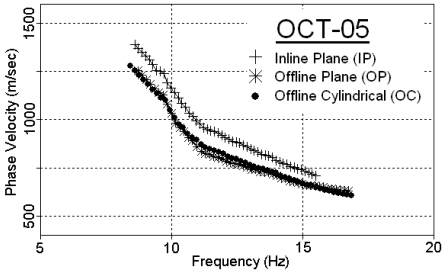

Fig. 6 Dispersion curves extracted from 24-channel linear array used during the field experiment in October 2005, obtained by using IP, OP, OC schemes.

CONCLUSIONS

With a roadside surface wave survey using a linear receiver array, it is recommended to use a 2D dispersion analysis scheme (despite the 1D nature of data acquisition) that accounts for the offline nature of the passive surface waves. In addition, considering a relatively long receiver array and the possibility of strong surface waves being generated at nearby points on the road, accounting for the circular wavefront through a simple modification of the 2D algorithm can improve the accuracy of the processing.

ACKNOWLEDGMENTS

Field experiments were made through careful preparations and precise operations performed by Brett Wedel, Noah Stimac, Larry Waldron, and Brett Bennett at the Kansas Geological Survey (KGS). We give our sincere appreciation to them.

REFERENCES

1. Lacoss, R.T., Kelly, E.J., and Toksöz, M.N., 1969, Estimation of seismic noise structure using arrays: Geophysics, **34**, 21-38.
2. Louie, J.N., 2001, Faster, better: shear-wave velocity to 100 meters depth from refraction microtremor arrays; Bulletin of the Seismological Society of America, 2001, **91**, (2), 347-364.
3. Okada, H., 2003, The microtremor survey method; Geophysical Monograph Series, no. 12, published by Society of Exploration Geophysicists (SEG), Tulsa, OK.
4. Park, C.B., Miller, R.D., Ryden, N., Xia, J., and Ivanov, J., 2005, Combined use of active and passive surface waves: *Journal of Engineering and Environmental Geophysics (JEEG)*, **10**, (3), 323-334.
5. Park, C.B., Miller, R.D., Xia, J., and Ivanov, J., 2004, Imaging dispersion curves of passive surface waves: SEG Expanded Abstracts: Soc. Explor. Geophys., (NSG 1.6), Proceedings in CD ROM.
6. Park, C.B., Miller, R.D., and Xia, J., 1999, Multichannel analysis of surface waves (MASW); Geophysics, **64**, 800-808.
7. Park, C.B., Xia, J., and Miller, R. D., 1998, Imaging dispersion curves of surface waves on multi-channel record; SEG Expanded Abstracts, 1377-1380.
8. Yoon, S., and Rix, G., 2004, Combined active-passive surface wave measurements for near-surface site characterization; Proceedings of the SAGEEP 2004, Colorado Springs, CO, SUR03, Proceedings on CD ROM.